VERTICAL STRUCTURE OF TURBULENCE IN OFFSHORE FLOW DURING RASEX

L. MAHRT*
College of Oceanic and Atmospheric Sciences, Oregon State University,Corvallis, OR 97331, U.S.A.

DEAN VICKERS
College of Oceanic and Atmospheric Sciences, Oregon State University,Corvallis, OR 97331, U.S.A.

JIM EDSON
Woods Hole Oceanographic Institute, Woods Hole, MA 02543, U.S.A.

JAMES M. WILCZAK
Environmental Technology Lab., ERL/NOAA, Boulder, CO 80303, U.S.A.

JEFF HARE
Cooperative Institute for Research in Environmental Sciences (CIRES), University of Colorado and Environmental Technology Lab., ERL/NOAA, Boulder, CO 80303, U.S.A.

JØRGEN HØJSTRUP
Risø National Laboratory, 4000 Roskilde, Denmark

(Received in final form 9 November 2000)

Abstract. The adjustment of the boundary layer immediately downstream from a coastline is examined based on two levels of eddy correlation data collected on a mast at the shore and six levels of eddy correlation data and profiles of mean variables collected from a mast 2 km offshore during the Risø Air-Sea Experiment. The characteristics of offshore flow are studied in terms of case studies and inter-variable relationships for the entire one-month data set. A turbulent kinetic energy budget is constructed for each case study.

The buoyancy generation of turbulence is small compared to shear generation and dissipation. However, weakly stable and weakly unstable cases exhibit completely different vertical structure. With flow of warm air from land over cooler water, modest buoyancy destruction of turbulence and reduced shear generation of turbulence over the less rough sea surface cause the turbulence to rapidly weaken downstream from the coast. The reduction of downward mixing of momentum by the stratification leads to smaller roughness lengths compared to the unstable case. Shear generation at higher levels and advection of stronger turbulence from land often lead to an increase of stress and turbulence energy with height and downward transport of turbulence energy toward the surface.

With flow of cool air over a warmer sea surface, a convective internal boundary layer develops downstream from the coast. An overlying relatively thick layer of downward buoyancy flux (virtual temperature flux) is sometimes maintained by shear generation in the accelerating offshore flow.

Keywords: Air-sea interaction, Coastal zone, Internal boundary layer, Sea surface stress, Turbulence energy.

* E-mail: mahrt@oce.orst.edu

Boundary-Layer Meteorology **100:** 47–61, 2001.

1. Introduction

The response of the atmosphere to surface discontinuities is often posed in terms of internal boundary layers (Garratt, 1990). In flow of warm air from a rough land surface over a cooler sea surface, the turbulence decreases due to a combination of stable stratification over the water and reduced surface roughness. The flow above the thin stable surface layer, which was part of the boundary layer over land, may become partially decoupled from the surface, accelerate and form a low-level wind maximum (Smedman et al., 1995; Tjernström and Smedman, 1993). The shear on the underside of the low-level wind maximum may eventually generate turbulence and re-establish a surface-based boundary layer. In this case, the main source of turbulence is elevated and not at the surface and Monin–Obukhov scaling does not apply (Smedman et al., 1995). Sun et al. (2000) show that close to the coast, advection from land dominates the near-surface stress.

Even without such decoupling, the reduction of surface roughness and surface stress over the sea can lead to a low-level wind maximum in offshore flow of warm air over cooler water (Garratt and Ryan, 1989). In a numerical study of the influence of the continental diurnal variation on offshore flow, Garratt (1987) found that the onset of daytime convective turbulence was advected offshore as a sharp horizontal change that could be traced for hundreds of kilometres offshore, well beyond the fetch in the present data. The numerical simulations of Mengelkamp (1991) indicate that the top of the stable internal boundary layer can be defined in terms of a minimum in the vertical profile of turbulence kinetic energy while numerical simulations of Garratt (1987) similarly indicate a minimum of eddy diffusivity at the top of the stable internal boundary layer. The level of minimum turbulence separates the underlying internal boundary layer from overlying decaying turbulence. In Mengelkamp (1991), this overlying decaying turbulence still exhibits some upward buoyancy flux offshore, characteristic of the upstream convective boundary layer.

A number of studies document the development of well-defined convective internal boundary layers in flow of cool air over a warm surface (see review in Garratt, 1990). The growing convective internal boundary layer is capped by a thin entrainment zone of downward buoyancy flux. In contrast, Sun et al. (1998) studied a convective internal boundary layer, which is capped by a relatively thick layer of downward buoyancy flux, maintained by elevated shear generation. The above studies suggest varied vertical structure of the convective internal boundary layer in offshore flow.

The present study analyzes offshore data from the Risø Air-Sea Experiment (RASEX). Using these data, Vickers and Mahrt (1999) found that close to the coast, modifications to Monin-Obukhov similarity theory may be required. Convective eddies are suppressed by the top of the thin internal boundary layer in unstable offshore flow. This partial suppression leads to larger nondimensional gradients and weaker fluxes than predicted by Monin-Obukhov similarity theory. For stable offshore flow, the nondimensional shear is smaller than predicted by the usual stability functions for Monin–Obkuhov similarity theory, particularly for young waves. In contrast, above the wave boundary layer (in which momentum transporting eddies are coherent with the surface waves) for stationary onshore flow, Monin–Obukhov scaling successfully describes the turbulence energy budget (Edson and Fairall, 1998; Wilczak et al., 1999) and the flux-gradient relationship (Vickers and Mahrt, 1999).

2. Data

We analyze offshore tower data collected during RASEX. The full instrumentation is described in Barthelmie et al. (1994) and Højstrup et al. (1997). In this study, we analyze observations taken at the sea mast west tower, located 2 km off the northwestern coast of the island of Lolland, Denmark, in 4 m of water, for the intensive observing period 3 October through 8 November 1994. The variation in mean water depth due to tides is only about 0.3 m. Local offshore (southerly) flow is characterized by a sea fetch ranging between 2 km and 5 km. Onshore flow has a fetch between 15 km and 25 km as it travels across an inland sea, and is still potentially fetch-limited. Fetch is the distance along the flow from the coast to the sea mast. Water depths for the longer fetches range from 4 m to 20 m. The nearby land surface is relatively flat farmland.

Various corrections to the data are recorded in Mahrt et al. (1996). Averaged vertical profiles of the buoyancy flux and friction velocity are computed from the six levels of sonic anemometers. In offshore flow, the vertical variation of the flux is much larger than differences between individual sonic anemometers. For some analyses, the fluxes for the three lowest levels will be averaged since the effect of instrumental differences may be larger than the actual vertical variation over such short vertical distances. The stability z/L for each record is computed from the fluxes averaged over the three lowest levels, where L is the Obukhov length. Insight into the vertical structure of the offshore flow can be gained by evaluating the turbulence kinetic energy budget using the stress and virtual temperature flux computed from sonic anemometers located at 3, 6, 10, 18, 32 and 45 m on the offshore tower.

For shear generation of turbulence kinetic energy, the mean wind shear is computed from seven cup anemometers (P224b sensor) located at 7, 15, 20, 29, 38, 43 and 48 m. Corrections to the cup anemometers are made by compositing the wind speed profile based on all of the records with fetch greater than 10 km and near-neutral conditions ($|z/L| < 0.1$). This averaged profile is fitted to a log-linear height-dependence and percentage corrections for each level are constructed from the deviation of the averaged profile from the log-linear fit. These corrections partially remove small systematic irregularities in the profile due to instrument error. Percentage corrections to the wind speed are always less than 2% but exert a greater influence on the shear. The computation of the shear-generation term neglects directional shear, which could not be adequately estimated from the sonic anemometer data due to small uncertainties in orientation.

For offshore cases (fetch <5 km), advection of turbulence kinetic energy is estimated as

$$V\left[\frac{TKE_{SM} - TKE_{LM}}{\text{fetch}}\right] \tag{1}$$

where SM refers to the offshore mast and LM refers to the land mast. This term can be estimated at the 6-m and 18-m levels, corresponding to the common sonic anemometer levels at the landmast and seamast. The wind speed V is taken from the appropriate level at the sea mast. Here, it is assumed that the turbulence kinetic energy, TKE, is spatially invariant along the coast for cases where the flow was not perpendicular to the coast. The above estimate of advection is probably an upper bound for the tower since the gradients are presumably strongest closer to the coast. Unfortunately, advection could not be estimated above 18 m.

Dissipation is estimated following the spectral approach of Edson and Fairall (1998). The spectral slope was determined from a least squares fit over the frequency range thought to be in the inertial subrange. In some cases, the inertial subrange does not appear to be fully developed, possibly due to nonequilibrium conditions in offshore flow and errors in the dissipation estimate. We expect the wave-induced pressure transport term to be small for these data even at the lowest (3-m) tower level (Hare et al., 1997). The wavelength and amplitude of the fetch-limited surface waves are generally small compared to open ocean values.

The residuals for the turbulence kinetic energy budget are expected to be large because the pressure transport term is neglected and the errors in the vertical flux divergence and horizontal advection of turbulence energy are expected to be significant. The vertical flux divergence of turbulence energy (triple correlation term) suffers larger random flux errors compared to covariances, and the flux divergence term is a small difference between vertical flux of turbulence energy at two levels. We have also neglected the Eulerian time-dependence, the mean vertical advection of turbulence kinetic energy and the horizontal flux divergence of turbulence energy. These terms appear to be small with relatively large errors.

3. Land-Sea Contrast

The maximum upward buoyancy flux at the sea surface most often occurs in the morning when the air advected from the land is coolest. The maximum downward buoyancy flux at the sea surface tends to occur in the late afternoon when the air over land is warmest. On average, the diurnal amplitude of the buoyancy flux is 0.02 K m s^{-1}. This averaged diurnal amplitude is small due to the low sun angle for 54° N in October and inclusion of numerous cloudy days in the average. Using temperature at two levels for summer for the same land and sea masts, Barthelmie et al. (1996) found, on average, stable conditions over the water during the day and unstable conditions at night.

For the data analyzed here, the stress at the seamast in offshore flow is, on average, half of the value over land. The flow typically accelerates by 1–2 m s^{-1} between land and the offshore mast. The roughness lengths over land (Barthelmie et al., 1996) are approximately 10 cm for southerly (offshore flow) and 5 cm for southeasterly flow where trajectories experience a mixture of land and sea. These roughness lengths are several orders of magnitude larger than those over the sea.

The buoyancy fluxes are relatively weak in this data set and the magnitude of z/L only occasionally exceeds 0.5. Nonetheless, the vertical structure of the flow is sensitive to whether the flow is weakly unstable or weakly stable. The greater sensitivity of the flow to stability, compared to over land (Section 4), may be due to coupling between the roughness length over the sea and the stability, as found in Plant et al. (1998). With stable conditions, the momentum flux to the sea surface is weaker. This corresponds to slower wave growth and smaller roughness compared to near-neutral and unstable cases.

To examine this relationship for the present data, roughness lengths were computed from the observed fluxes from individual one-hour records using the Paulson-Dyer stability functions. The roughness lengths were then averaged for different intervals of z/L. As a second calculation, roughness lengths were computed from fluxes, which were first averaged for different intervals of z/L before computing the roughness length. Both methods showed a sharp decrease of the roughness length with increasing stability. For the second method, the roughness length calculated from 3-m data decreases systematically from 10^{-4} m for near-neutral conditions to values several orders of magnitude smaller for large stability. As a result, the influences of stability and roughness change on the offshore flow are coupled and the overall effect of stability is enhanced compared to that over land. This problem is currently being investigated with eddy correlation and wave data from multiple sites. Inaccuracy of the Dyer stability function does not seem to be the cause of the correlation between the roughness lengths and stability.

For the relationships examined in subsequent sections, the characteristics of the offshore flow are more systematically related to travel time than fetch in terms of the scatter, suggesting that the flow is influenced by an internal decay time scale. The turbulence may decay more near the surface where the travel time to the tower is longer (weaker wind near the surface) and the dissipation time scale is shorter (smaller turbulent length scale near the surface). For offshore flow, the travel times at the offshore mast generally range between a few hundred seconds and about 600 seconds. The decay time of convective turbulence can be estimated in terms of the ratio of the vertical length scale of the turbulence divided by the velocity scale of the turbulence. Nieuwstadt and Brost (1986) and Sorbjan (1997) provide specific formulations for the case where the velocity scale is the free convection velocity and the length scale is the depth of the convective mixed layer. Applying such a

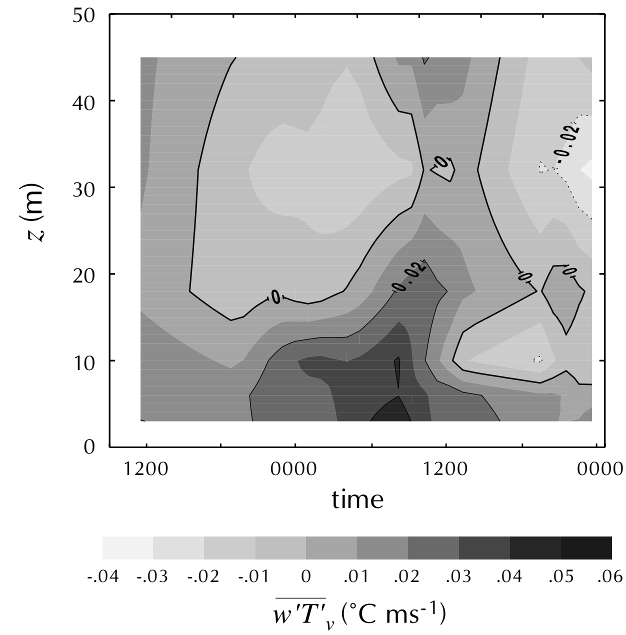

Figure 1. Time-height cross-section for weakly unstable case UI for the buoyancy flux (°C m s^{-1}) where darker areas correspond to upward buoyancy flux. Times are GMT which is one hour behind local solar time.

relationship to the RASEX cases with convective conditions over land predicts a decay time scale on the 'order' of ten minutes, which is consistent with the observed variation of turbulence quantities with travel time over the sea found in Section 4.

4. Upward Buoyancy Flux from the Sea Surface

We now study the flow of cool air over the warmer sea surface in terms of the three periods when the buoyancy flux at the surface exceeds 0.01 K m s^{-1} for more than a half day (Table I). All three cases are characterized by very weak instability. The time-height cross-section for the case of longest duration (Figure 1) shows diurnal variation with maximum upward buoyancy flux in the morning due to advection of cool air from land.

The turbulence energy budget is averaged over all of the one-hour records within each case. Averaging over nonstationary periods does not correspond to an ensemble average. However, the individual one-hour budgets are noisier, especially with respect to the smaller terms in the turbulence kinetic energy budget. The residuals of the averaged turbulence energy budgets (Figure 2) are reasonably small considering the expected substantial errors in certain terms of the budget and

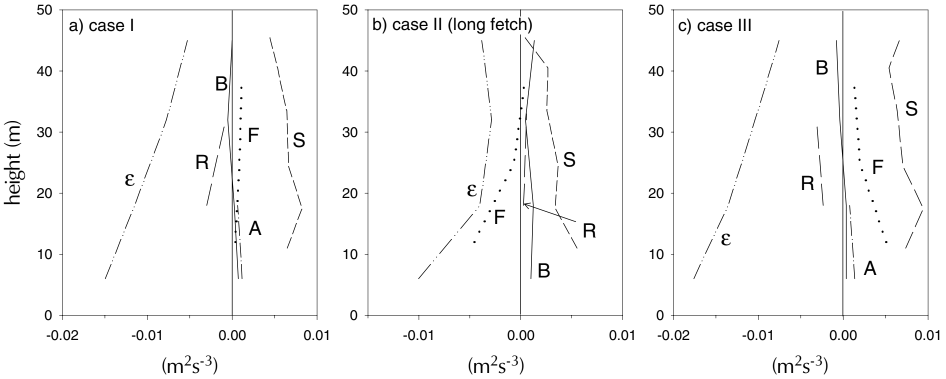

Figure 2. The turbulence energy budget ($m^2\ s^{-3}$) for the slightly unstable cases. A is the advection term, ϵ the dissipation, S the shear-generation term, F the vertical divergence of the flux of the turbulence energy and B the buoyancy-generation term. The residual, R, is computed from the two levels where all the terms can be evaluated.

TABLE I

Case Studies: B.F. is the buoyancy flux ($K\ m\ s^{-1}$) averaged over the 3, 6 and 10 m levels, 'travel' refers to the travel time in minutes, fetch is in kilometres and V is the 10 m wind speed. Case I for the stable and unstable flows include time-height cross-sections of the buoyancy flux (Figures 1 and 4).

Case study	Time (DOY)	Travel	Fetch	B.F.	Wind ($m\ s^{-1}$)	z/L
Unstable-UI	291.9–293.0	5	3	0.02	10	−0.10
Unstable-UII	289.25–290	35	18	0.03	9	−0.11
Unstable-UIII	307.7–308.35	4.5	2.8	0.01	10	−0.02
Stable-SI	297.0–297.7	5	2	−0.02	7	0.44
Stable-SII	299.0–301.0	6	2.8	−0.01	8	0.06
Stable-SIII	303.15–303.25	5	2	−0.01	6.5	0.11

omission of the pressure transport term (Section 2). Error bars for the averaged profiles are not shown because much of the variation within the averaging period is due to either diurnal trend or other nonstationarity, rather than random variations. In addition to the three case studies, this section analyses statistics based on all of the individual one-hour records within the entire field program when $z/L < -0.1$.

The buoyancy-generation of turbulence energy is quite small compared to the shear generation and dissipation (Figure 2), although this weak buoyancy flux strongly influences the vertical structure, as discussed below. For unstable conditions, the horizontal advection of turbulence energy is also small in the turbulence energy budget, at least near the surface where it could be evaluated (Figures 2a, c).

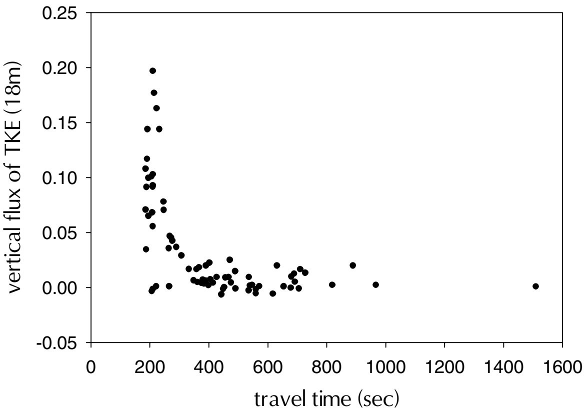

Figure 3. The dependence of the vertical flux of turbulence energy (m^3 s^{-3}) at 18 m on travel time for all of the one-hour records with fetch values less than 5 km for unstable conditions ($z/L < -0.1$).

Horizontal advection presumably becomes increasingly important at higher levels and also shoreward of the seamast.

For the two short fetch cases, the vertical flux convergence is positive near the surface (Figure 2), which would be consistent with the fact that the tower occupies the bulk of the thin developing internal boundary layer. For Case UII, the flow reaches the tower after a relatively long fetch of 18 km and travel time of about 35 min. The vertical flux divergence term is negative near the surface corresponding to traditional export of turbulence energy upward out of the surface layer. The flow is unstable at all levels and the momentum flux is approximately constant with height, within the uncertainty due to differences between different sonic anemometers. These observations imply that the internal boundary layer is deep compared to the tower layer. The buoyancy flux is small and erratic for this case due to small air-sea temperature difference resulting from the longer fetch.

The layer of upward buoyancy flux is capped by a layer of downward buoyancy, which sometimes is as thick as, or thicker than, the layer of upward buoyancy flux. This vertical structure is seen in the first part of Figure 2, after which the depth of the convective layer grows and engulfs the entire tower layer. In the former case, the vertically integrated buoyancy flux is small or even negative and the vertically-integrated turbulence is driven by shear generation.

The turbulent transport of turbulence energy (Figure 3) is often large upward for unstable cases with short travel time of less than 300 s where advection from land is most important. The turbulent transport is never significant downward. For stable offshore flow, the pattern is quite different (next section).

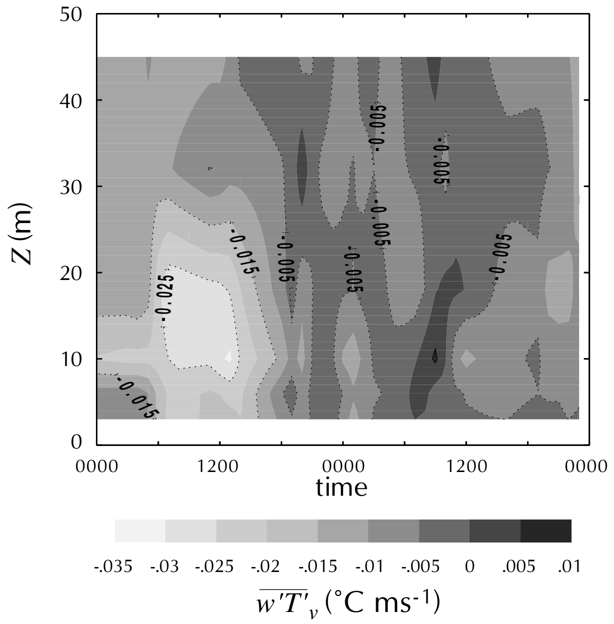

Figure 4. Time-height cross-section of the buoyancy flux (°C m s^{-1}) for weakly stable case SI where lighter areas correspond to stronger downward buoyancy flux. Times are GMT which is one hour behind local solar time.

5. Downward Buoyancy Flux

Flow of warm air over a cooler surface is now analyzed in terms of three case study periods where the magnitude of the downward buoyancy flux at the surface is greater than 0.01 K m s^{-1} for most of the episode. The time-height cross-section for the buoyancy flux is shown for the case with the largest sustained downward buoyancy flux (Figure 4). For this case, the downward buoyancy flux at the sea surface is due to advection of warm air from the heated land surface over the cooler water and exhibits significant diurnal variation. The vertical structure of the turbulence kinetic energy budget is averaged for all of the one-hour records in each of the three cases (Figures 5a–c). All three cases correspond to short fetch, short travel time (Table I) and weak stability. We will also analyze statistics based on all of the individual one-hour records during the entire field program when $z/L > 0.1$.

5.1. Elevated stress maximum

For stable periods, the stress often increased with height (Vickers and Mahrt, 1999). This occurred for even weak stability but was more pronounced for the few cases of stronger stability, as in Figure 6, where the measured stress and downward heat flux near the surface have essentially collapsed, within measurement error. This

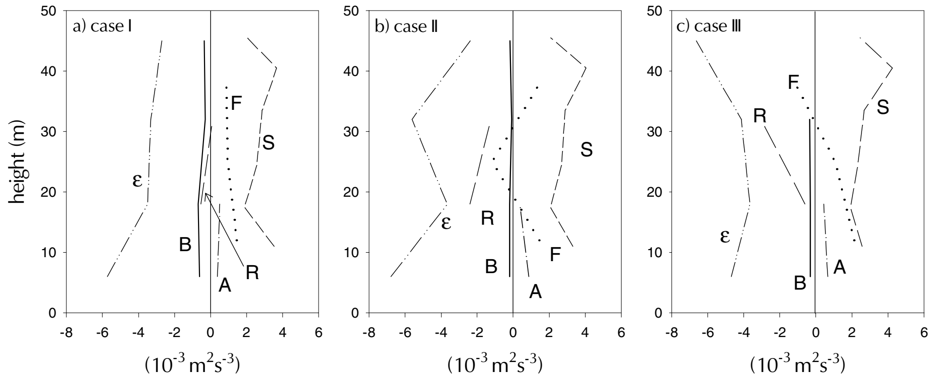

Figure 5. The turbulence energy budget (10^{-3} m^2 s^{-3}) for the three weakly stable Cases (a–c). A is the advection term, ϵ the dissipation, S the shear-generation term, F the vertical divergence of the flux of the turbulence energy, B the buoyancy-generation term and R, the residual.

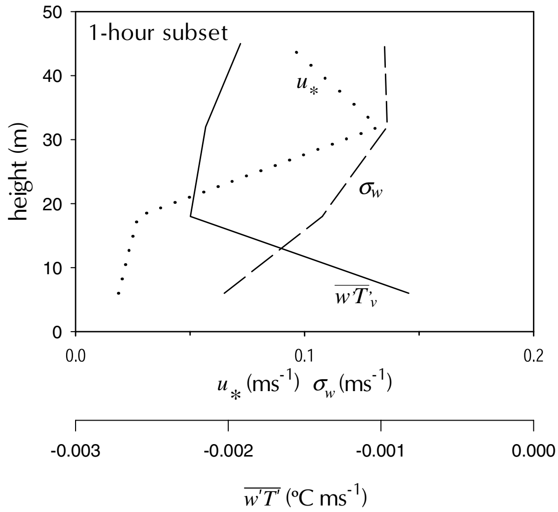

Figure 6. Vertical profiles of the friction velocity (m s^{-1}), buoyancy flux (°C m s^{-1}) and σ_w (m s^{-1}) for a one-hour period during case SI where surface fluxes are very weak.

vertical structure is quite different from observed traditional stable boundary layers where the stress, buoyancy flux and turbulence energy decrease monotonically with height (Caughey et al., 1979; Lenschow et al., 1987; Sorbjan, 1988). In the present observations of offshore flow, the elevated maxima of stress and turbulence energy are maintained by shear generation and presumably augmented by advection of stronger turbulence from land.

The stress convergence below the elevated stress maximum acts to accelerate the flow and may account for much of the observed flow acceleration downstream from the coast. The observed vertical convergence of stress at the sea mast, applied over the travel time from the coast, corresponds to an acceleration of 0.5–1.0 m s^{-2}. The observed acceleration ranged from 0.8–1.3 m s^{-2}. A rigorous assessment of the momentum budget is prevented by inadequate assessment of the local horizontal pressure gradient.

The observed increase of stress with height does not appear to be related to instrumentation differences. For long-fetch, near-neutral conditions, the observed stress is essentially constant with height across the tower layer (or decreases very slowly with height), as expected in non-advective traditional boundary layers where the boundary layer is much deeper than the tower layer.

An elevated stress maximum is also observed by Glendening (2000) in a large eddy simulation model of flow from a rough surface to a smooth surface with zero buoyancy flux. He used this elevated stress maximum to define the top of the new internal boundary layer. The elevated maximum was maintained by horizontal advection. Definition of the top of the internal boundary layer in terms of a stress maximum contrasts sharply with definition of the top of the internal boundary layer in terms of a minimum of turbulence, cited in the Introduction.

To form a simple measure of the vertical structure of the stress for individual records, the ratio of stress in the upper part of the tower layer to that in the lower part of the tower layer, is computed as:

$$\text{stress ratio} = \frac{\text{stress}_{\text{upper}}}{\text{stress}_{\text{lower}}}, \tag{2}$$

where $\text{stress}_{\text{upper}}$ is the average of the stress magnitude at the two upper tower levels, 32 m and 45 m, and $\text{stress}_{\text{lower}}$ is the average of the three lowest levels, 3 m, 6 m and 10 m. This ratio is computed for all of the one-hour records where $z/L > 0.1$. The momentum flux ratio is sometimes large for small travel time, exceeding two in a significant fraction of the cases (Figure 7). These values correspond to a rapid increase of stress with height. The momentum flux ratio decreases rapidly with increasing travel time to values closer to unity for travel times of ten minutes and longer, although the scatter is large. For values near unity, the stress changes slowly with height, implying that the internal boundary layer is deep compared to the tower layer.

What generates this vertical structure? Firstly, the shear-generation term tends to increase with height (Figure 5), in contrast to the usual boundary layer where it decreases rapidly with height. Secondly, the turbulence advected horizontally from land in offshore flow is thought to decay more slowly at higher levels where the turbulence length scale is larger. The dissipation rate divided by the turbulence energy decreases with height for both stable and unstable cases. Finally, the advection of stress might increase with height due to increasing wind speed with height.

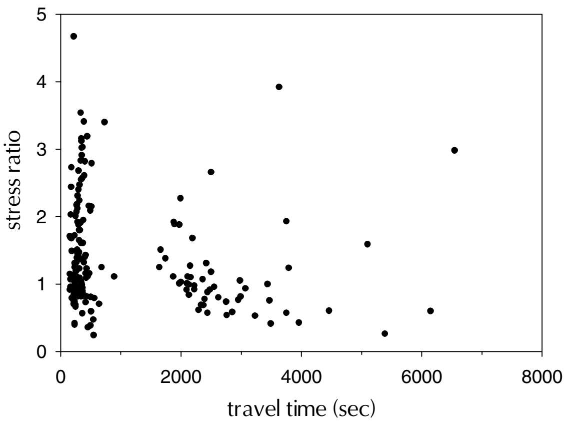

Figure 7. The stress ratio (Equation (2)) as a function of travel time for all of the one-hour records with stable conditions ($z/L > 0.1$).

5.2. Downward transport of turbulence

For Cases SI and SIII, the vertical turbulent transport of turbulence kinetic energy is significant downward (not shown), implying that the main source of turbulent kinetic energy is elevated and the near surface flow is a sink of turbulence energy. This downward transport of turbulence energy is consistent with the increase of turbulence and stress with height. The downward transport of turbulence kinetic energy leads to significant vertical flux convergence of turbulence energy at the lower levels (Figure 5). The turbulence near the surface is therefore partly maintained by downward transport of turbulence energy. The downward transport of turbulence toward the surface may be augmented by the pressure transport term in the turbulence kinetic energy equation (Smedman et al., 1995), not evaluated here.

Considering all of the stable one-hour records, the vertical transport of turbulence energy for short travel times is often large positive (Figure 8), as also occurred in the unstable offshore flow cases. However, in contrast to unstable conditions, the vertical transport of turbulence energy is sometimes large downward for short travel times less than 300 s (Figure 8), again implying that the main source of turbulence is elevated in some stable offshore flows. These cases of downward transport of turbulence energy normally correspond to an increase of stress with height (Figure 9, momentum flux ratio >1). Our attempts to model this type of ‘boundary layer’ have not been successful to date.

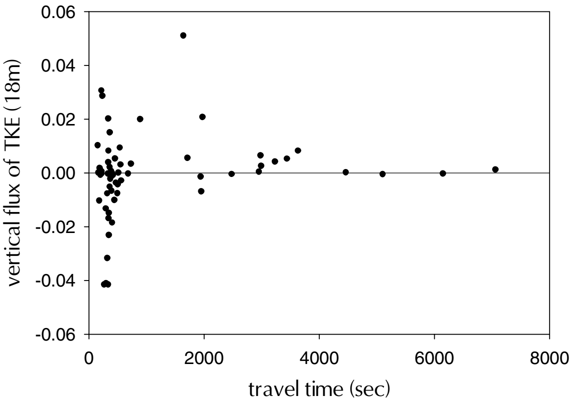

Figure 8. The dependence of the vertical flux of turbulence energy ($m^3\ s^{-3}$) at 18 m on travel time for all of the one-hour records with stable conditions ($z/L > 0.1$).

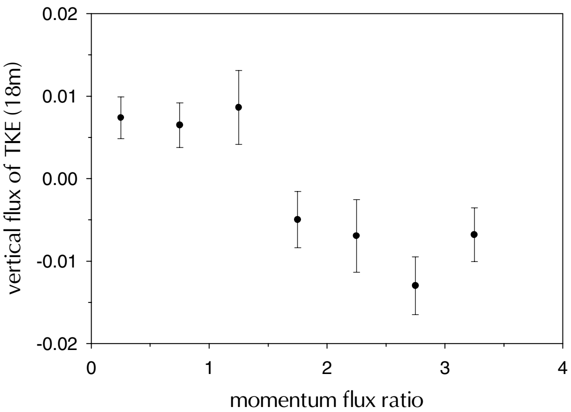

Figure 9. The relationship between the turbulence energy flux ($m^3\ s^{-3}$) at 18 m and the momentum flux ratio for stable conditions based on bin-averaged values computed from the one-hour records. Also shown are standard error bars.

6. Conclusions

For the present data, weakly convective internal boundary layers in flow of cooler air over warmer water are sometimes capped by a relatively thick layer of downward buoyancy flux. In such cases, the vertically-integrated buoyancy flux is small or even negative and the vertically-integrated turbulence is driven by shear generation and possibly horizontal advection.

With advection of warm air over cooler water, the vertical structure may be quite different even though the flow is normally only weakly stable ($z/L < 0.5$).

These cases often occur in the afternoon with flow of warm air from the heated land surface. In some cases, the turbulence energy and stress increase with height, reaching an elevated maximum, and the transport of turbulence energy is downward toward the surface, in contrast to unstable conditions. This structure was observed with travel times less than 10 minutes (fetches generally less than 5 km). The increase of stress with height appears to be maintained by horizontal advection of stronger turbulence from land and shear generation associated with accelerating flow over the water.

The downward transport of turbulence kinetic energy over the sea implies that the net generation of turbulence over the water surface is much weaker than over the upstream land surface due to a combination of stability and reduced surface roughness over the sea. These two effects are not separable in that stable stratification restricts the downward transport of momentum to the sea surface, which leads to smaller surface roughness lengths. Consequently, the overall effect of the buoyancy flux is greater than that over land where the roughness length is essentially constant. The relationship between the roughness length and the stability may contribute to the large differences in vertical structure of the flow for the cases of weak upward and weak downward buoyancy flux, which occur even though the buoyancy term in the turbulence kinetic energy equation is small compared to shear production and dissipation.

Acknowledgements

We gratefully acknowledge the important comments of anonymous reviewers and the computational assistance of Sesha Sadagopan. This material is based upon work supported by Grant N0001409810282 from the Office of Naval Research, Marine Meteorology.

References

Barthelmie, R. J., Courtney, M. S., Højstrup, J., and Sanderhoff, P.: 1994, *The Vindeby Project: A Description*, Report R-741(EN), Risø National Laboratory, DK4000, Roskilde, Denmark.

Barthelmie, R. J., Grisogono, B., and Pryor, S. C.: 1996, 'Observations and Simulations of Diurnal Cycles of Near-Surface Wind Speeds over Land and Sea', *J. Geophys. Res.* **101**, 21,327–21,337.

Caughey, S. J., Wyngaard, J. C., and Kaimal, J. C.: 1979, 'Turbulence in the Evolving Stable Boundary Layer', *J. Atmos. Sci.* **36**, 1041–1052.

Edson, J. and Fairall, C. W.: 1998, 'Similarity Relationships in the Marine Atmospheric Surface Layer for Terms in the TKE and Scalar Variance Budgets', *J. Atmos. Sci.* **55**, 2311–2328.

Garratt, J. R.: 1987, 'The Stably Stratified Internal Boundary Layer for Steady and Diurnally Varying Offshore Flow', *Boundary-Layer Meteorol.* **38**, 369–394.

Garratt, J. R.: 1990, 'The Internal Boundary Layer – a Review', *Boundary-Layer Meteorol.* **50**, 171–203.

Garratt, J. R. and Ryan, B. F.: 1989, 'The Structure of the Stably Stratified Internal Boundary Layer in Offshore Flow over the Sea', *Boundary-Layer Meteorol.* **47**, 17–40.

Glendening, J.: 2000, 'Turbulent Characteristics of Internal Boundary Layers', in *Fourteenth Symposium on Boundary Layers and Turbulence*, Aspen, CO, U.S.A., Amer. Meteorol. Soc., pp. 15–18.

Hare, J. E., Hara, T., Edson, J. B., and Wilczak, J. M.: 1997, 'A Similarity Analysis of the Structure of Airflow over Surface Waves', *J. Phys. Oceanog.* **27**, 1018–1037.

Højstrup, J., Edson, J., Hare, J., Courtney, M. S., and Sanderhoff, P.: 1997, 'The RASEX 1994 Experiments', Risø -R-788, Risø National Laboratory, Roskilde, Denmark (ISBN-87-550-2039-9), 24 pp.

Lenschow, D. H., Li, X. S., Zhu, C. J., and Stankov, B. B.: 1987, 'The Stably Stratified Boundary Layer over the Great Plains. I. Mean and Turbulence Structure', *Boundary-Layer Meteorol.* **42**, 95–121.

Mahrt, L., Vickers, D., Howell, J., Højstrup, J., Wilczak, J. A., Edson, J., and Hare, J.: 1996, 'Sea Surface Drag Coefficients in RASEX', *J. Geophys. Res.* **101**, 14327–14335.

Mengelkamp, H.-T.: 1991, 'Boundary Layer Structure over an Inhomogeneous Surface: Simulation with a Non-Hydrostatic Mesoscale Model', *Boundary-Layer Meteorol.* **57**, 323–342.

Nieuwstadt, F. and Brost, R.: 1986, 'The Decay of Convective Turbulence', *J. Atmos. Sci.* **43**, 532–546.

Plant, W., Keller, W. Hesany, V., and Hayes, K.: 1998: 'Measurements of the Marine Boundary Layer from an Airship', *J. Atmos. Oceanic. Tech.* **15**, 1433–1458.

Smedman, A.-S., Bergström, H., and Högström, U.: 1995,'Spectra, Variances and Length Scales in a Marine Stable Boundary Layer Dominated by a Low Level Jet', *Boundary-Layer Meteorol.* **76**, 211–232.

Sorbjan, Z.: 1988, 'Structure of the Stably-Stratified Boundary Layer during the SESAME-1979 Experiment', *Boundary-Layer Meteorol.* **44**, 255–266.

Sorbjan, Z.: 1997, 'Decay of Convective Turbulence Revisited', *Boundary-Layer Meteorol.* **82**, 501–515.

Sun, J., Desjardins, R., Mahrt, L., and MacPherson, J. I.: 1998, 'Transport of Carbon Dioxide, Water Vapor and Ozone by Turbulence and Local Circulations', *J. Geophys. Res.* **103**, 25,873–25,885.

Sun, J., Vandemark, D., Mahrt, L., Vickers, D., Crawford, T., Vogel, C., and Dumas, E.: 2000, 'Momentum Transfer over the Coastal Zone', *J. Geophys. Res.*, in press.

Tjernström, M. and Smedman, A.-S.: 1993, 'The Vertical Structure of the Coastal Marine Atmospheric Boundary Layer', *J. Geophys. Res.* **98**, 4809–4826.

Vickers, D. and Mahrt, L.: 1999, 'Observations of Nondimensional Shear in the Coastal Zone', *Quart. J. Roy. Meteorol. Soc.*, **125**, 2685–2702.

Wilczak, J., Edson, J., Højstrup, J., and Hara, T.: 1999, 'The Budget of Turbulent Kinetic Energy in the Marine Atmospheric Surface Layer', in G. L. Geernaert (ed.), *Air-Sea Exchange: Physics, Chemistry, and Dynamics*, Kluwer Academic Publishers, Dordrecht, Boston, pp. 153–174.